2342

Dynamics of the second order nonlinearity in thermally-poled silica-glass

D. Faccio, V. Pruneri
Corning-OTI R&D, Viale Sarca 222, 20126 Milano, Italy
P.G. Kazansky
Optoelectronics Research Centre, Southampton University, Southampton, SO17 1BJ, UK

Abstract: We study the temporal evolution of the second-order nonlinearity in thermally poled silica-glass. Our results differ significantly from those reported so far for the ionic charge evolution and show strong dependencies on sample thickness.

OCIS codes: (060.4370) Nonlinear optics, fibers; (060.2280) Fiber design and fabrication

Ever since its first demonstration, thermal poling as a means of inducing a second-order nonlinearity (SON) in glass has attracted much interest due to its potential applications in various optical devices. It is a well established fact that in glass the mechanism at the basis of SON formation is ionic migration and subsequent creation of a frozen-in internal electric field. However, theoretical modeling of field-assisted ion migration is rather complex and has been limited to one [1] or two species [2] whereas experimental evaluation of positive-ion movement [3] may not be sufficient to determine the exact internal electric-field profile. Here we investigate the temporal evolution of the nonlinear coefficient (d_{33}) and of the nonlinear thickness (L) in thermally poled silica using the noncollinear Makers fringe technique (NCMFT) which allows high resolution [4]. Samples of different thickness (S) were thermally poled for various poling times. The silica-glass samples were Herasil 1 grade (from Heraeus) with $S = 1$, 0.5 and 0.1 mm. Thermal poling was performed at $270°C$ in air by applying a constant voltage (V) of 4kV, using Al-evaporated electrodes, for seven different times (t): 2, 5, 10, 20, 30, 45 and 90 minutes. The samples were subsequently cooled to room temperature with the voltage still applied. Cooling from $270°C$ to $200°C$ (when poling effects become negligible) takes ~ 40 seconds.

The nonlinear depth was obtained using the NCMFT which allows non-destructive measurements of thicknesses as small as 2 μm with sub-micron resolution [4]. Two identical input fundamental beams are focused onto the sample with a relative $90°$ external angle. The power of the generated noncollinear second harmonic (SH) beam is measured as a function of the sample inclination angle and L is estimated by fitting the spacing and position of the observed peaks with the function given in [4]. The measurements were carried out using a Q-switched and mode-locked Nd:YAG laser as fundamental source. A half-wave plate controls the polarisation of the fundamental pulses before they are split by a 50% beam-splitter and focused onto the sample. The SH signal was measured with a photo-multiplier tube after eliminating the fundamental beam using broadband and interferometric filters. Figure 1(a) shows an example of the SH power as a function of inclination angle for a sample with $S = 0.5$ mm and poled for 10 minutes, along with the best fit obtained assuming a truncated-gaussian nonlinear profile $\propto s(L) \cdot \exp[-(z - L/4)^2/L^2]$ where s(z)=1 if $0 < z < L$ and is otherwise null and in this particular case $L = 3.4$ μm, as shown in the inset of the figure. The sharp decrease in the profile may be due to the presence of a thin charge layer. Once L is known the nonlinear coefficient is found by normalising the collinear SH with respect to that from a reference sample (quartz) and assuming that the tensorial components of the nonlinearity d_{33} and d_{31} are related to each other by $d_{33} = 3d_{31}$. All measurements were made one hour after poling and then repeated a week later without observing any significant variation in the measured L or d values. Figure 1(b) shows the observed evolution of the nonlinear coefficient d_{33}. A fast initial increase is followed by a significant decrease to a final value which is roughly 50% smaller than the peak-d_{33}. Furthermore, the poling times for which the peak-d_{33} values are observed decrease with decreasing S.

The main mechanism for the nonlinearity formation is thought to be electric-field induced ion migration - after cooling the sample and removing the electrodes an electric field (E) remains frozen in the sample that couples with the third-order nonlinearity to give an effective SON,

$$d_{33} = \frac{3}{2}\chi^{(3)}E \qquad (1)$$

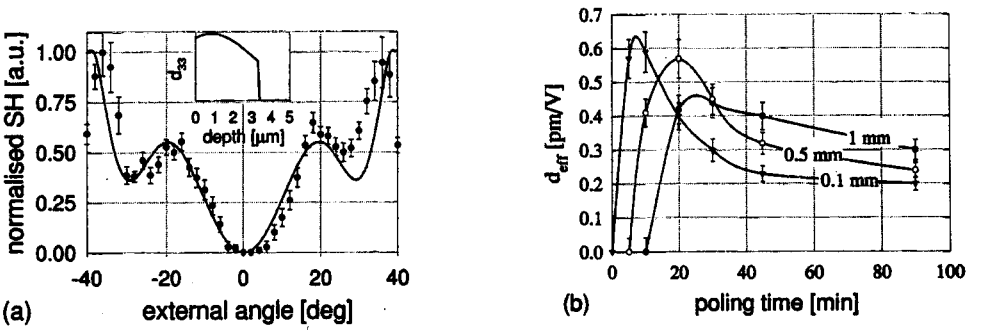

Fig. 1. (a) Example of noncollinear Makers fringe measurement on a 0.5 mm thick Herasil 1 sample thermally poled at 280^oC, 4 kV, 10 minutes. Circles - experimental data. Solid line - best fit obtained using $L = 3.4$ μm. (b) Experimental values for the nonlinear coefficient (d_{33}) against poling time for samples of different thickness (S): $S = 1$ mm - full circles; $S = 0.5$ mm - open circles; $S = 0.1$ mm - full triangles. The lines are only a guide for the eye.

where $\chi^{(3)}$ is the glass third-order nonlinear susceptibility and E is the frozen-in electric field. The full equations which describe this process, considering both drift and diffusion, can be rather complicated and have been solved under simplified conditions. Von-Hippel [1] considered only one ion species drifting which, in our case, would be sodium (Na^+), the main charge carrier in silica-glass with mobility μ_{Na}. As the thermally mobilised ions drift towards the cathode, two distinct regions form in the glass: a depleted region with negative space-charge followed by an un-depleted, neutral region. The depletion region forms under the anode with a monotonically increasing depth, until the equilibrium value $L_\infty = \sqrt{2\varepsilon V/\rho}$ is reached (where ε is the glass dielectric constant and ρ the depleted charge density). The internal voltage drop also increases with t and the overall effect is an increase in the frozen-in electric field, i.e. in d_{33}, and the maximum value is reached at equilibrium. Therefore a one-charge carrier model cannot account for our experimental results which show a fast growth to a maximum followed by a slower decrease to smaller values.

The next most mobile charge carrier in silica glass is H^+ with a mobility (μ_H) which has been found to be in the range 10^{-4}-10^{-3} μ_{Na}. If press-contact or non-blocking evaporated electrodes are used, then hydrogen continuously diffuses under the influence of the externally applied electric field from the external atmosphere into the glass. Due to the fact that $\mu_H \ll \mu_{Na}$ three regions will form: straight under the anode a region with Na^+ substituted by H^+ - the charge in this region will depend on the amount of in-diffused H^+. This is followed by a negatively charged depletion layer and finally by the un-depleted neutral region. It is worth noting at this point that this model is still an approximation of the true situation. Indeed, the Na^+-depleted region is very different from the un-treated glass: the most mobile charge carriers have been removed and an electric field close to dielectric breakdown value is applied. Under these conditions a non-ohmic electronic current is to be expected. However, in its simplicity, the as-described two-charge carrier model provides a valuable insight to thermal poling.

The equations describing the process have been solved by Alley et al. [2] - the electric field inside the sample initially rises but is then followed, for longer poling times, by a decrease to smaller values. The nonlinear coefficient, proportional to the electric field, will follow the same evolution. It is worth noting that the above model describes thermal poling in air: poling in vacuum or with blocking electrodes shows a different behaviour [2, 5]. As we were able to ascertain using a similar model, the poling times for which the maximum d_{33} values are obtained depend on many parameters, such as ion concentrations and mobilities which vary from glass to glass. Most importantly, there is a strong dependence on S due to the higher electric-field values inside the thinner samples thus explaining the results in figure 1(b). Figure 1(b) also shows that there seems to be a minimum poling time below which no SH is observed (also observed in [2]). This minimum poling time is smaller than 40 seconds (necessary to apply the voltage and cool the sample) for $S = 0.1$ mm but increases to 5 minutes for $S = 0.5$ mm and to 10 minutes for $S = 1$ mm. Furthermore, poling at a higher temperature (e.g. 280^oC) resulted in a shift of these threshold times to smaller values (2 minutes for $S = 0.5$ mm and 5 minutes for $S = 1$ mm). These results may be explained by assuming that the time required for a charge distribution to form, such that SH generation can occur, depends on both temperature and sample thickness (maybe due to a reduced mixed-ion mobility near the cathode [2]). By raising the temperature (i.e. ionic mobility) or decreasing the sample thickness (i.e. increasing the applied electric field) the necessary

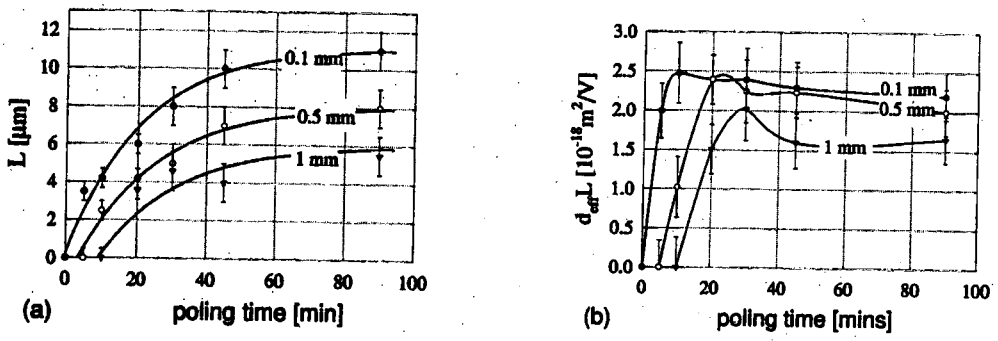

Fig. 2. (a) Experimental values for the nonlinear thickness L and (b) product $d_{33}L$ of the measured nonlinear coefficient and thickness against poling time for three sample thicknesses. $S = 0.1$ mm - full circles, $S = 0.5$ mm - open circles, $S = 1$ mm - full triangles. The lines in (a) are the best stretched-exponential fits for the experimental data and in (b) are only a guide for the eye.

charge distributions are achieved for smaller poling times.

Figure 2(a) shows the evolution of L for the same samples of fig.1(b). The well-known continuous increase in L is observed (see e.g. ref.[5]). The lines show the best fits for functions of the form

$$L(t) = L(0) + \alpha(1 - e^{-\beta t}) \tag{2}$$

where $L(0) + \alpha = L(\infty)$ is the saturation value and β is the growth rate. The observed evolution of L differs (in particular for S=0.1 mm) from the measured positive ion-charge front evolution ($\propto \ln(t)$) [2] implying that the actual value of the nonlinear thickness may not correspond to that expected from these measurements. It is well known that a depletion region a few microns thick forms in the first seconds of poling [3] but we may infer from our measurements that another mechanism (maybe electronic migration) is necessary in order to also observe SHG and to explain the differences between positive-charge-distribution and SH measurements. Figure 2(a) also shows a marked dependence on sample thickness which may be qualitatively assigned to the different electric fields inside the samples.

Figure 2(b) shows the product $d_{33}L$ against poling time. The growth rates vary according to the sample thickness but the saturation value is roughly the same ($\simeq 2.4 \cdot 10^{-18}$ m^2/V) for all S. This value may be used to estimate the $\chi^{(3)}$ using eq (1) and assuming that all the applied 4 kV voltage drops across the depletion region and remains constant. In this case we find $\chi^{(3)} = 4 \cdot 10^{-22}$ m^2/V^2, in good agreement with values estimated by other means [6].

References

1. A. Von Hippel, Phys. Rev., Opt. Lett. , **91**(3), 568-579 (1953).
2. T.G. Alley, S.R.J. Brueck and R.A. Myers, J. Non-Cryst. Sol., **242**, 165-176 (1998).
3. T.G. Alley, S.R.J. Brueck and M. Wiedenbeck, J. Appl. Phys., **86**(12), 6634-6640 (1999).
4. D. Faccio, V. Pruneri and P.G. Kazansky, Opt. Lett., **25**(18), 1376-1378 (2000).
5. V. Pruneri, F. Samoggia, G. Bonfrate, P.G. Kazansky and G.M. Yang Appl. Phys. Lett. **74**(17), 2423-2425 (1999).
6. D. Wong, W. Xu, S. Fleming and M. Janos, Opt. Fibre Techn. **5**, 235-241 (1999).